Brief communication

Variable skeletal phenotypes associated with biallelic variants in *PRKG2*

The 100 000 Genomes Project (100KGP) is a UK-wide initiative that has a goal of using whole genome sequencing (WGS) to identify genetic causes of rare inherited diseases and embed the use of this technology within the NHS.[1] Using data from this resource alongside international gene-matching efforts, four individuals from two independent families were identified harbouring homozygous frameshift or stop-gain variants in *PRKG2*, a recently described skeletal dysplasia gene.[2] Detailed clinical and radiological assessments helped extend the phenotypic range associated with this autosomal recessive condition while functional studies indicated that both variants had a similar impact on FGF-induced MAPK signalling.

PRKG2 encodes the cyclic guanosine monophosphate dependent protein kinase II (cGKII), which acts downstream of the natriuretic peptide receptor-B/C- natriuretic peptide (NPR-B/CNP). NPR-B is encoded by *NPR2*, biallelic variants in which are responsible for acromesomelic dysplasia, Maroteaux type (AMDM; MIM 602875). Rodent models further implicate PRKG2 in skeletal development[3 4] and cGKII deficiency was shown to be the cause of the dwarfism phenotype observed in Angus cattle.[5] Building on support from pathway analysis and model organisms, a recent study showed that biallelic *PRKG2* variants can result in acromesomelic dysplasia, PRKG2-type (AMDP) in humans,[2] adding *PRKG2* to a list of >400 genes associated with genetic skeletal disorders.[6] As only two affected individuals were reported, it is important that the full clinical range of this condition is described.

In this study, we searched for rare biallelic *PRKG2* variants using data from the 100KGP via the LabKey application available within Genomic England's research environment. Researchers can apply for access online (www.genomicsengland.co.uk/join-a-gecip-domain). Initial filtering employed a 1% population allele frequency threshold based on data from the 1000 Genomes Project as well as in-house frequency information. An additional family was identified via a network of collaborators and variants were classified using ACMG criteria (online supplemental table 1).

In family 1, WGS and subsequent Sanger sequencing uncovered a homozygous pathogenic *PRKG2* variant, NM_006259.3:c.2282dup (p.Asp761Glufs*34; online supplemental figure 1) in three brothers referred with spondylometaphyseal dysplasia (figure 1A). Interestingly, the middle-affected brother (F1-IV-6) also has type I osteogenesis imperfecta (OI). An early clinical exome sequencing study found that for 4.6% of cases with a molecular diagnosis, more than one gene was contributing to a blended phenotype.[7] Complex cases such as these are expected to be more common in highly consanguineous families where large regions of homozygosity (ROHs) make up a significant proportion of the genome; however, for F1-IV-6 the secondary diagnosis of OI was due to a *COL1A1* frameshift, which had arisen *de novo*. OI was suspected in this child because of multiple fractures in childhood (arm as an infant, wrist aged 8 and thoracic T6 wedge fracture) combined with blue sclerae. It is certainly possible that the coexistent OI may have had an impact on the severity of the phenotype in this individual, not least because his height was more significantly reduced than for his two brothers and OI (type 1) is a known cause of reduced stature in its own right.

In family 2, exome sequencing for a girl with acromesomelic dysplasia revealed a homozygous pathogenic *PRKG2* variant c.1705C>T; p.(Arg569*) (online supplemental figure 2), observed previously in a patient with similar clinical and radiological features.[2] Comparison of the available genomic data for F2-V-3 and the previously published case was not able to detect a shared haplotype across the *PRKG2* locus. However, exome sequencing has limited resolution to detect small regions of identity by descent and so a founder mutation cannot be ruled out. Given the differing ethnicities and the fact that c.1705C>T lies at a CpG dinucleotide, the recurrence of c.1705C>T being due to separate mutational events seems a more likely scenario.

Both variants described here are extremely rare; p.(Asp761Glufs*34) is absent from gnomAD (https://gnomad.broadinstitute.org), while p.(Arg569*) is present as a singleton allele. In both families, the disease-causing variants lay within large ROHs (online supplemental table 2). Pathogenic variants are overrepresented in the largest ROHs and it has been proposed that lying in one of the top 10 such regions can be used as evidence supporting pathogenicity.[8] While the p.(Arg569*) variant has already been demonstrated to affect the downstream MAPK pathway,[2] the p.(Asp761Glufs*34) in family 1 is likely to be disruptive given the switch of the final Asp-Phe residues for 33 alternative amino acids at the C terminus. *In silico* modelling highlights the structural importance of this region, in particular the final Phe762 residue (figure 1B, supplementary methods; interactive version at https://michelanglo.sgc.ox.ac.uk/r/prkg2).

To functionally confirm the pathogenicity of the newly identified p.(Asp761Glufs*34) variant, we first analysed cGKII expression by western blot analysis. Plasmid construction for p.(Asp761Glufs*34) involved a sequential PCR strategy (supplemental methods), with the previously characterised p.(Arg569*) variant employed as a positive control. For both variants, cGKII was detected at the predicted size (figure 1C), although at dramatically reduced levels (≥80%) compared with the wild type (figure 1D). Next, we evaluated whether the p.Asp761Glufs*34 mutant was able to inhibit FGF2-induced MAPK pathway by analysing its ability to induce phosphorylation of Raf-1 at Ser-43 and ERK1/2, as described previously.[2] Wild-type cGKII downregulated MAPK signalling by reducing ERK1/2 activation through the upstream phosphorylation of Raf-1 at Ser-43 in a cGMP-dependent manner. However, the p.Asp761Glufs*34 mutant failed to phosphorylate Raf-1 at Ser-43 and thus, reduced FGF2-induced ERK1/2 phosphorylation (figure 1E–F), similar to results for the p.Arg569* variant.[2]

Detailed phenotypic information is provided for both families and compared with the two published cases (online supplemental table 2, figure 3). Radiological findings for F2-V-3 were very similar to those observed for 'Proband 1' described previously,[2] which is unsurprising given that both individuals harbour the same homozygous p.(Arg569*). In contrast, for *PRKG2* family 1 there was a consistent radiological phenotype distinct from previously reported AMDP and AMDM. The three brothers reported here (F1-IV-3, IV-6 and IV-7) had no evidence of acromesomelic shortening, except for mild shortening of toes observed for individual F1-IV-7. The main findings were platyspondyly with anterior vertebral body projections, long slender femoral necks and some metaphyseal irregularity (most evident in the radius and ulna) and striations (figure 2). The metaphyses of the distal phalanges were somewhat cone-shaped in one child, but not

J Med Genet: first published as 10.1136/jmedgenet-2021-108027 on 15 November 2021. Downloaded from http://jmg.bmj.com/ on October 19, 2022 at UCL Library Services. Protected by copyright.

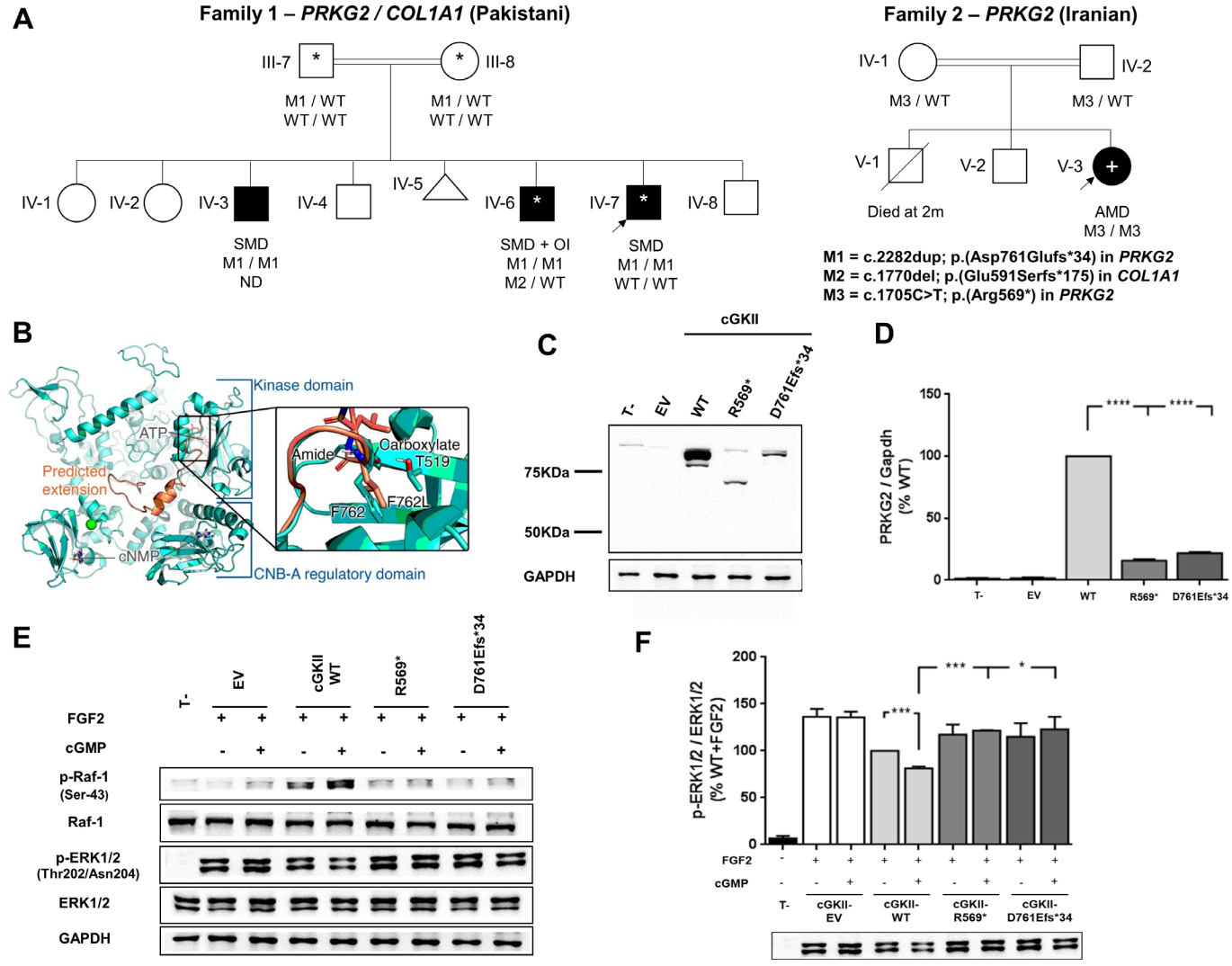

Figure 1 Pedigrees, structural modelling and the effects of the *PRKG2* variants on cGKII protein levels/MAPK pathway regulation. (A) Simplified pedigrees and segregation of variants in *PRKG2* and *COL1A1* in two families with rare skeletal dysplasias. More detailed pedigrees are shown in online supplemental figure 4. AMD, acromesomelic dysplasia (mild); ND, not determined; OI, osteogenesis imperfecta; SMD, spondylometaphyseal dysplasia; WT, wild-type; *, WGS performed as part of 100KGP; +, exome sequencing. The *COL1A1* variant was initially detected by targeted sequencing in 2011 but confirmed to have arisen *de novo* by WGS. (B) Structure of cGKII (wild type: turquoise) with overlay of the mutant, p.Asp761Glufs*34 (salmon) extension and inset of Phe762 residue. The protein kinase domain is regulated by two cyclic nucleotides binding (CNB) domains. The predicted C-terminal extension would fall between CNB-A domain and the protein kinase domain and is likely to interfere with the activation of the latter by the former, were it to be stable, a conclusion not supported by *in silico* predictions. In fact, the extension results in a deleterious amino acid change of a core residue, Phe762, to a leucine (inset). Also visible is the hydrogen bond between the terminal carboxylate and Thr519, whereas the amide bond between Leu762 and Leu763 is forced away in order to best accommodate the subsequent residues. (C) Immunoblotting results for cGKII (upper panel) and GAPDH as an endogenous control (lower panel) of cell lysates extracted from transiently transfected HEK293T cells. Both human cGKII mutants as well as wild-type (WT) proteins were detected at their predicted size: R569*: 65.1 kDa and D761Efs*34: 91.1 kDa (calculated by using the ExPaSy online tool, https://web.expasy.org). (D) Densitometry quantification of cGKII showing that there is an 80% reduction in expression of the two mutants compared with WT. (E) Western blots of phosphorylated Raf-1 and ERK1/2 proteins of the MAPK pathway showed that neither of the mutants were able to phosphorylate c-Raf at Ser43 and therefore downregulate ERK activation compared with WT in response to FGF2 induction in transiently transfected HEKT293 cells. (F) Densitometry quantification of pMAPK 44/42 protein revealed that neither R569* nor D761Efs*34 mutants were able to downregulate FGF2-induced ERK1/2 activation compared with WT, in transiently transfected HEK293 cells in the presence of 8-pCPT-cGMP. Three biological experiments were performed, and significance values are represented as *p<0.05, **p<0.01, ***p<0.001 and ****p>0.0001. EV, empty vector; T–, untransfected cells.

pronounced, generalised or associated with shortening, as seen in AMDM.[9] In summary, family 1 exhibited a skeletal phenotype characterised by spondylometaphyseal dysplasia, rather than acromesomelic dysplasia as expected in AMDP and AMDM.

Interestingly, the *PRKG2* locus has been identified in several genome-wide association studies on height (www.ebi.ac.uk/gwas/genes/PRKG2). Therefore, the description of this now confirmed Mendelian condition constitutes an additional example of rare variants in a gene causing a severe condition, where common variants in the same gene are associated with a related trait.[10] In summary, analysis of 100KGP data combined with gene-matching efforts identified four affected individuals with biallelic loss of function variants in *PRKG2*, extending the

J Med Genet: first published as 10.1136/jmedgenet-2021-108027 on 15 November 2021. Downloaded from http://jmg.bmj.com/ on October 19, 2022 at UCL Library Services. Protected by copyright.

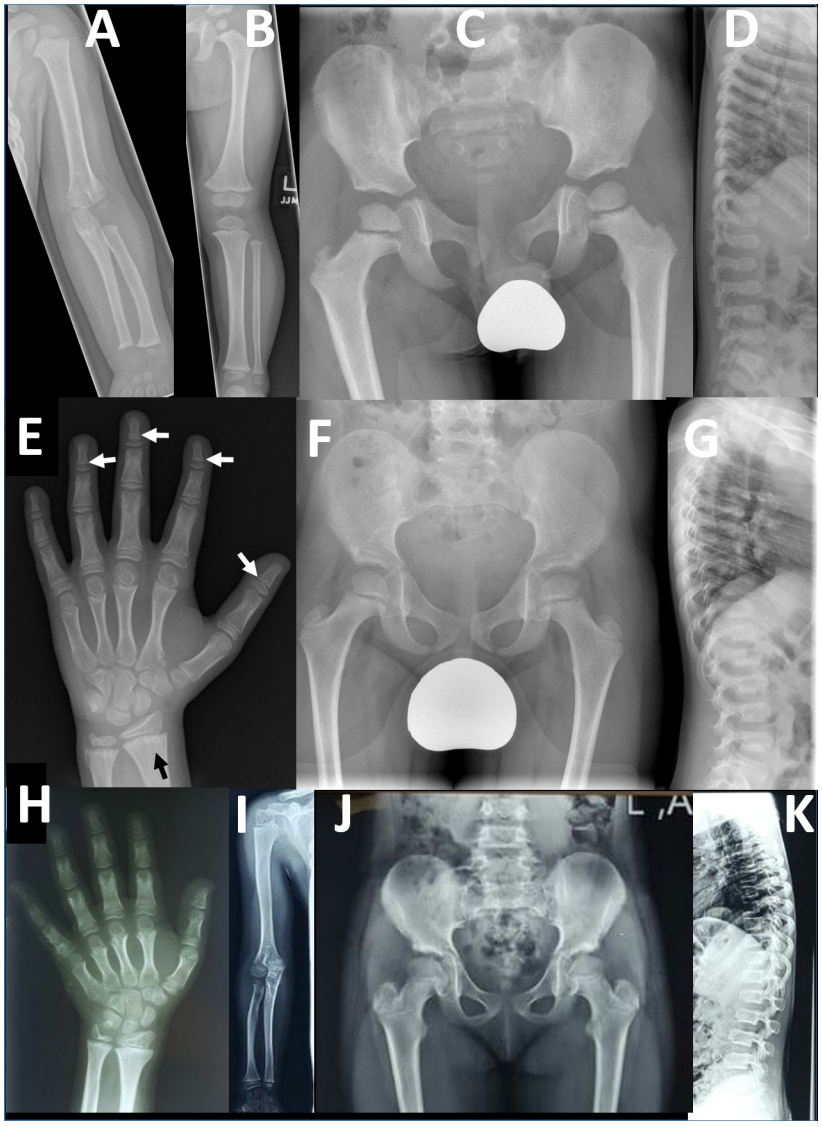

Figure 2 Radiographic findings in two families with *PRKG2* variants: radiographs of left upper limb (A) and lower limb (B) in a 26-month-old boy (F1-IV-7) from family 1. The long bones are stocky in appearance but there is no disproportion within the limbs. (C) Pelvic radiograph at age 4 in same child shows development of long, slender femoral necks. (D) Lateral spinal radiograph at age 4 show generalised mild platyspondyly with small central anterior projections of the vertebral bodies, and hypoplasia of the L2 vertebral body. (E) Left hand radiograph at age 11 in same child shows no brachydactyly; there is mild metaphyseal chondrodysplasia evident in the distal radius and particularly the ulna, with some metaphyseal striations (black arrow); subtle coning of the distal phalangeal metaphyses is evident (white arrows), without associated shortening. Pelvic (F) and lateral spine (G) radiographs in middle affected sibling (F1-IV-6) in family 1 showing similar features of long slender femoral necks and platyspondyly with anterior vertebral body projections. Osteopaenia is also evident; this child also has type 1 osteogenesis imperfecta due to a *de novo* pathogenic variant in *COL1A1*. Additional radiology is available for F1-IV-3 in online supplemental figure 5 which shows similar results to those for F1-IV-7. (H) Left hand radiograph in female child (F2-V-3, aged 10 years) from family 2 showing generalised brachydactyly. (I) Right upper limb radiograph also from F2-V-3 demonstrates mild disproportionate shortening of the radius and ulna relative to the humerus (mesomelic shortening). (J) Pelvic radiograph from F2-V-3 demonstrates mildly elongated femoral necks. (K) Lateral spine radiograph from the same individual demonstrates mild platyspondyly with small anterior vertebral body projections.

phenotypic range of this condition to include spondylometaphyseal dysplasia. The patients described here were the only individuals harbouring severe biallelic *PRKG2* variants across all rare disease areas within the 100KGP. These data include 295 patients recruited due to an unexplained skeletal dysplasia and therefore our results are consistent with this condition being extremely rare in humans.

Alistair T Pagnamenta ,[1,2] **Francisca Diaz-Gonzalez** ,[3] **Benito Banos-Pinero,**[4] **Matteo P Ferla,**[1,2] **Mehran B Toosi,**[5] **Alistair D Calder,**[6] **Ehsan G Karimiani,**[7,8] **Mohammad Doosti,**[8] **Andrew Wainwright,**[9] **Paul Wordsworth,**[1,2,9] **Kathryn Bailey,**[9] **Katarina Ejeskär,**[10] **Tracy Lester,**[4] **Reza Maroofian,**[11] **Karen E Heath** ,[3,12] **Homa Tajsharghi,**[10] **Deborah Shears,**[13] **Jenny C Taylor,**[1,2] **The Genomics England Research Consortium**

[1]NIHR Biomedical Research Centre, Oxford, UK
[2]Wellcome Centre for Human Genetics, Oxford University, Oxford, UK
[3]INGEMM, IdiPAZ and Skeletal Dysplasia Multidisciplinary Unit (UMDE, ERN-BOND), Hospital Universitario La Paz, Madrid, Spain
[4]Oxford Genetics Laboratories, Oxford University Hospitals NHS Foundation Trust, Oxford, UK
[5]Department of Pediatric Neurology, Ghaem Hospital, Mashhad University of Medical Sciences, Mashhad, Iran
[6]Radiology Department, Great Ormond Street Hospital for Children NHS Foundation Trust, London, UK
[7]Genetics Research Centre, Molecular and Clinical Sciences Institute, St. George's, University of London, London, UK
[8]Next Generation Genetic Polyclinic, Razavi International Hospital, Mashhad, Iran
[9]Department of Paediatrics, Oxford University Hospitals NHS Foundation Trust, Oxford, UK
[10]School of Health Sciences, Translational Medicine, University of Skövde, Skövde, Sweden
[11]Department of Neuromuscular Disorders, Queen Square Institute of Neurology, UCL, London, UK
[12]CIBERER, ISCIII, Madrid, Spain
[13]Oxford Centre for Genomic Medicine, Oxford University Hospitals NHS Foundation Trust, Oxford, UK

Correspondence to Dr Deborah Shears; debbie.shears@ouh.nhs.ukDr Jenny C Taylor; jenny@well.ox.ac.uk

Acknowledgements We thank the two families for their involvement in our study. This research was made possible through access to the data and findings generated by the 100,000 Genomes Project. The 100KGP is managed by Genomics England Limited (a wholly owned company of the Department of Health and Social Care). The 100KGP uses data provided by patients and collected by the National Health Service as part of their care and support.

Collaborators The Genomics England Research Consortium (27th May 2021): John C. Ambrose (Genomics England, London, UK); Prabhu Arumugam (Genomics England, London, UK); Roel Bevers (Genomics England, London, UK); Marta Bleda (Genomics England, London, UK); Freya Boardman-Pretty (Genomics England, London, UK, William Harvey Research Institute, Queen Mary University of London, London, EC1M 6BQ, UK); Christopher R Boustred (Genomics England, London, UK); Helen Brittain (Genomics England, London, UK); Mark J Caulfield (Genomics England, London, UK, William Harvey Research Institute, Queen Mary University of London, London, EC1M 6BQ, UK); Georgia C Chan (Genomics England, London, UK); Greg Elgar (Genomics England, London, UK, William Harvey Research Institute, Queen Mary University of London, London, EC1M 6BQ, UK); Tom Fowler (Genomics England, London, UK); Adam Giess (Genomics England, London, UK); Angela Hamblin

J Med Genet: first published as 10.1136/jmedgenet-2021-108027 on 15 November 2021. Downloaded from http://jmg.bmj.com/ on October 19, 2022 at UCL Library Services. Protected by copyright.

(Genomics England, London, UK); Shirley Henderson (Genomics England, London, UK, William Harvey Research Institute, Queen Mary University of London, London, EC1M 6BQ, UK); Tim J P Hubbard (Genomics England, London, UK); Rob Jackson (Genomics England, London, UK); Louise J Jones (Genomics England, London, UK, William Harvey Research Institute, Queen Mary University of London, London, EC1M 6BQ, UK); Dalia Kasperaviciute (Genomics England, London, UK, William Harvey Research Institute, Queen Mary University of London, London, EC1M 6BQ, UK); Melis Kayikci (Genomics England, London, UK); Athanasios Kousathanas (Genomics England, London, UK); Lea Lahnstein (Genomics England, London, UK); Sarah E A Leigh (Genomics England, London, UK); Ivonne U S Leong (Genomics England, London, UK); Javier F Lopez (Genomics England, London, UK); Fiona Maleady-Crowe (Genomics England, London, UK); Meriel McEntagart (Genomics England, London, UK); Federico Minneci (Genomics England, London, UK); Loukas Moutsianas (Genomics England, London, UK, William Harvey Research Institute, Queen Mary University of London, London, EC1M 6BQ, UK); Michael Mueller (Genomics England, London, UK, William Harvey Research Institute, Queen Mary University of London, London, EC1M 6BQ, UK); Nirupa Murugaesu (Genomics England, London, UK); Anna C Need (Genomics England, London, UK, William Harvey Research Institute, Queen Mary University of London, London, EC1M 6BQ, UK); Peter O'Donovan (Genomics England, London, UK); Chris A Odhams (Genomics England, London, UK); Christine Patch (Genomics England, London, UK, William Harvey Research Institute, Queen Mary University of London, London, EC1M 6BQ, UK); Mariana Buongermino Pereira (Genomics England, London, UK); Daniel Perez-Gil (Genomics England, London, UK); John Pullinger (Genomics England, London, UK); Tahrima Rahim (Genomics England, London, UK); Augusto Rendon (Genomics England, London, UK); Tim Rogers (Genomics England, London, UK); Kevin Savage (Genomics England, London, UK); Kushmita Sawant (Genomics England, London, UK); Richard H Scott (Genomics England, London, UK); Afshan Siddiq (Genomics England, London, UK); Alexander Sieghart (Genomics England, London, UK); Samuel C Smith (Genomics England, London, UK); Alona Sosinsky (Genomics England, London, UK, William Harvey Research Institute, Queen Mary University of London, London, EC1M 6BQ, UK); Alexander Stuckey (Genomics England, London, UK); Mélanie Tanguy (Genomics England, London, UK); Ana Lisa Taylor Tavares (Genomics England, London, UK); Ellen R A Thomas (Genomics England, London, UK, William Harvey Research Institute, Queen Mary University of London, London, EC1M 6BQ, UK); Simon R Thompson (Genomics England, London, UK); Arianna Tucci (Genomics England, London, UK, William Harvey Research Institute, Queen Mary University of London, London, EC1M 6BQ, UK); Matthew J Welland (Genomics England, London, UK); Eleanor Williams (Genomics England, London, UK); Katarzyna Witkowska (Genomics England, London, UK, William Harvey Research Institute, Queen Mary University of London, London, EC1M 6BQ, UK); Suzanne M Wood (Genomics England, London, UK, William Harvey Research Institute, Queen Mary University of London, London, EC1M 6BQ, UK).

Contributors ATP and JCT conceived the project. ATP, BB-P, MPF, FD-G, TL, RM and KEH performed data analysis. BB-P and FD-G generated experimental data. The 57 members of GERC performed WGS and provided access data via a secure research environment. MBT, ADC, EGK, MD, AW, PW, KB, KE, RM, HT and DS recruited the patients and collected/interpreted clinical information. ATP drafted the manuscript, which was revised and approved by all.

Funding This research was supported by the National Institute for Health Research (NIHR) Oxford Biomedical Research Centre Programme, the Wellcome Trust (203141/Z/16/Z) and the European Union's Seventh Framework Programme for research, technological development and demonstration under grant agreement no. 608473 (to HT). Additional support was from MINECO grant no. SAF2017-84646-R from (to KEH) and via an FPU studentship (to FD-G) from the Spanish Ministry of Education. The 100KGP is funded by the National Institute for Health Research and NHS England. The Wellcome Trust, Cancer Research UK and the Medical Research Council have also funded research infrastructure.

Competing interests None declared.

Patient consent for publication Consent obtained from parent(s)/guardian(s)

Ethics approval The 100K Genomes Project has approval from the HRA Committee East of England (Cambridge South REC: 14/EE/1112).

Provenance and peer review Not commissioned; externally peer reviewed.

Supplemental material This content has been supplied by the author(s). It has not been vetted by BMJ Publishing Group Limited (BMJ) and may not have been peer-reviewed. Any opinions or recommendations discussed are solely those of the author(s) and are not endorsed by BMJ. BMJ disclaims all liability and responsibility arising from any reliance placed on the content. Where the content includes any translated material, BMJ does not warrant the accuracy and reliability of the translations (including but not limited to local regulations, clinical guidelines, terminology, drug names and drug dosages), and is not responsible for any error and/or omissions arising from translation and adaptation or otherwise.

OPEN ACCESS

Open access This is an open access article distributed in accordance with the Creative Commons Attribution 4.0 Unported (CC BY 4.0) license, which permits others to copy, redistribute, remix, transform and build upon this work for any purpose, provided the original work is properly cited, a link to the licence is given, and indication of whether changes were made. See: https://creativecommons.org/licenses/by/4.0/.

© Author(s) (or their employer(s)) 2022. Re-use permitted under CC BY. Published by BMJ.

► Additional material is published online only. To view please visit the journal online (http://dx.doi.org/10.1136jmedgenet-2021-108027)

Check for updates

To cite Pagnamenta AT, Diaz-Gonzalez F, Banos-Pinero B, *et al*. *J Med Genet* 2022;**59**:947–950.

Received 14 June 2021
Accepted 8 October 2021
Published Online First 15 November 2021

J Med Genet 2022;**59**:947–950.
doi:10.1136/jmedgenet-2021-108027

ORCID iDs
Alistair T Pagnamenta http://orcid.org/0000-0001-7334-0602
Francisca Diaz-Gonzalez http://orcid.org/0000-0003-1364-7586
Karen E Heath http://orcid.org/0000-0002-5816-7044

REFERENCES

1 Turnbull C, Scott RH, Thomas E, Jones L, Murugaesu N, Pretty FB, Halai D, Baple E, Craig C, Hamblin A, Henderson S, Patch C, O'Neill A, Devereau A, Smith K, Martin AR, Sosinsky A, McDonagh EM, Sultana R, Mueller M, Smedley D, Toms A, Dinh L, Fowler T, Bale M, Hubbard T, Rendon A, Hill S, Caulfield MJ, O'Neill A, Genomes P, 100 000 Genomes Project. The 100 000 Genomes Project: bringing whole genome sequencing to the NHS. BMJ 2018;361:k1687.
2 Díaz-González F, Wadhwa S, Rodriguez-Zabala M, Kumar S, Aza-Carmona M, Sentchordi-Montané L, Alonso M, Ahmad I, Zahra S, Kumar D, Kushwah N, Shamim U, Sait H, Kapoor S, Roldán B, Nishimura G, Offiah AC, Faruq M, Heath KE. Biallelic cGMP-dependent type II protein kinase gene (*PRKG2*) variants cause a novel acromesomelic dysplasia. J Med Genet 2022;59:28–38.
3 Pfeifer A, Aszódi A, Seidler U, Ruth P, Hofmann F, Fässler R. Intestinal secretory defects and dwarfism in mice lacking cGMP-dependent protein kinase II. Science 1996;274:2082–6.
4 Tsuchida A, Yokoi N, Namae M, Fuse M, Masuyama T, Sasaki M, Kawazu S, Komeda K. Phenotypic characterization of the Komeda miniature rat Ishikawa, an animal model of dwarfism caused by a mutation in Prkg2. Comp Med 2008;58:560–7.
5 Koltes JE, Mishra BP, Kumar D, Kataria RS, Totir LR, Fernando RL, Cobbold R, Steffen D, Coppieters W, Georges M, Reecy JM. A nonsense mutation in cGMP-dependent type II protein kinase (PRKG2) causes dwarfism in American Angus cattle. Proc Natl Acad Sci U S A 2009;106:19250–5.
6 Mortier GR, Cohn DH, Cormier-Daire V, Hall C, Krakow D, Mundlos S, Nishimura G, Robertson S, Sangiorgi L, Savarirayan R, Sillence D, Superti-Furga A, Unger S, Warman ML. Nosology and classification of genetic skeletal disorders: 2019 revision. Am J Med Genet A 2019;179:2393–419.
7 Yang Y, Muzny DM, Xia F, Niu Z, Person R, Ding Y, Ward P, Braxton A, Wang M, Buhay C, Veeraraghavan N, Hawes A, Chiang T, Leduc M, Beuten J, Zhang J, He W, Scull J, Willis A, Landsverk M, Craigen WJ, Bekheirnia MR, Stray-Pedersen A, Liu P, Wen S, Alcaraz W, Cui H, Walkiewicz M, Reid J, Bainbridge M, Patel A, Boerwinkle E, Beaudet AL, Lupski JR, Plon SE, Gibbs RA, Eng CM. Molecular findings among patients referred for clinical whole-exome sequencing. JAMA 2014;312:1870–9.
8 Wakeling MN, Laver TW, Wright CF, De Franco E, Stals KL, Patch A-M, Hattersley AT, Flanagan SE, Ellard S, Study DDD, DDD Study. Homozygosity mapping provides supporting evidence of pathogenicity in recessive Mendelian disease. Genet Med 2019;21:982–6.
9 Wang W, Song MH, Miura K, Fujiwara M, Nawa N, Ohata Y, Kitaoka T, Kubota T, Namba N, Jin DK, Kim OH, Ozono K, Cho T-J. Acromesomelic dysplasia, type Maroteaux caused by novel loss-of-function mutations of the NPR2 gene: three case reports. Am J Med Genet A 2016;170A:426–34.
10 Freund MK, Burch KS, Shi H, Mancuso N, Kichaev G, Garske KM, Pan DZ, Miao Z, Mohlke KL, Laakso M, Pajukanta P, Pasaniuc B, Arboleda VA. Phenotype-specific enrichment of Mendelian disorder genes near GWAS regions across 62 complex traits. Am J Hum Genet 2018;103:535–52.

J Med Genet: first published as 10.1136/jmedgenet-2021-108027 on 15 November 2021. Downloaded from http://jmg.bmj.com/ on October 19, 2022 at UCL Library Services. Protected by copyright.

Table S2: Clinical details and variant information for four individuals from two independent families with biallelic variants in *PRKG2*. Results are compared to two cases reported by Díaz-González *et al* 2020. Sequencing methods in Family 2 are as described by Pagnamenta *et al* 2021. NA, not available; ROH, region of homozygosity. Variant annotation is based on NM_006259.3. SDs for adults heights were calculated using https://tall.life/height-percentile-calculator-age-country. For Family 1 we used the mean adult height obtained from the Royal College of Paediatrics and Child Health's standard growth chart.

	Families reported here				**Díaz-González *et al* 2020**	
Family/individual ID	**Family 1**			**Family 2**	**Proband 1**	**Proband 2**
Consanguinity (parental relationship)	Yes (double 1st cousins)			Yes (double 2nd cousins)	Yes (3rd cousins)	Yes (3rd cousins)
Ethnicity	Pakistani			Iranian	Moroccan	Indian
Parents' stature	Father 177 cm (0 SD); Mother 160 cm (-0.60 SD)			Father 155 cm (-2.10 SD); Mother 171 cm (1.90 SD)	Father 165 cm (-1.75 SD); Mother 164 cm (-0.01 SD)	Father 158 cm (-2.59 SD); Mother 147 cm (-2.50 SD)
Individual	IV-3	IV-6	IV-7	V-3	II-2	II-2
Gender (M/F)	M	M	M	F	F	F
Age at first referral	13 years	8 months	2 years	3 years	NA	4 years
Referral reason	Diagnosis due to sibling	Poor weight gain, unusual limb proportions, hypotonia, large head	Short stature	Short stature/dysmorphism	Short stature/suspected skeletal dysplasia	Short stature/suspected skeletal dysplasia
Homozygous variant	c.2282dupA; p.(Asp761Glufs*34)			c.1705C>T; p.(Arg569*)	c.1705C>T; p.(Arg569*)	c.491dupA; p.(Asn164Lysfs*2)
Allele Frequency (gnomAD 2.1.1)	Absent			1/250704	1/250704	Absent
ROH region GRCh38 (size, rank)	NA	chr4:25,732,624-85,677,887 (60.0Mb, #1)	chr4:53,687,014-85,677,887 (32.0Mb, #3)	chr4: 30,724,365-89,247,731 (58.5Mb)	NA	NA
Hypotonia	NA	Yes	N/A	No	-	-
Birth weight	2700 g	N/A	N/A	3350 g	NA	NA
Birth length	N/A	N/A	N/A	50 cm	NA (−1.93 SDS at 3 weeks)	NA
Birth OFC	N/A	N/A	N/A	34 cm	NA (−0.42 SDS at 3 weeks)	NA
Developmental milestones	Normal	Normal	Normal	Normal	Normal	Normal
Growth / feeding	No concerns until 4y	Poor feeder	NA	Normal	NA	NA
Age at last assessment (years)	26	22	15	10	12	11
Height (Percentile/SD)	158.5 cm (-2.5 SD)	140.8 cm (-4.9 SD)	143.8 cm (-3.11 SD)	121 cm (-2.5 SD)	-4.01 SD	−5.06 SD
Sitting height (cm)	85	76	77	70	NA	NA
Leg length	NA	-2 to -3 SD	NA	53	NA	NA
Skeletal proportions	Mild rhizomelia of upper and lower limbs	Moderate rhizomelia of upper and lower limbs	Mild rhizomelia of upper and lower limbs	Rhizomelic shortening of the upper and lower extremities.	Mild mesomelic shortening of the limbs (lower limbs, radius and ulna); sitting height to height ragio was 0.579 (1.21 SDs)	No (upper to lower segment ratio 1.41 aged 11y)
OFC (centile)	50-75th	50-75th	50-75th	56cm	-	-
Kyphosis	Yes, mild, thoracic region	Yes, mild, mid-thoracic	-	No	-	-
Digital anomalies	Normal except for broad thumbs and short 4-5th metacarpels	Normal except for broad thumbs	-	Short, broad fingers	Short, stubby fingers	Short stubby fingers
Acromelia	No	No	No	No	-	-
Feet	Flat feet	NA	Mild shortening of toes (Figure S3A bottom)	Short broad toes	-	Sandal gap
Facial appearance	Normal	Triangular face, when younger	Normal	Broad nasal bridge, thick eyebrows, synophrys, prominent chin	Normal	Triangular face, broad nasal bridge, pointed chin, synophrys, hypertelorism, low set ears.
Cranial findings	NA	Multiple Wormian bones	NA	Normal	Normal	Normal
Palate	Normal	Normal	Normal	Normal	-	-
Platyspondyly	Yes	Yes	Yes (mild)	Yes	Yes (mild flattening of the thoracic vertebral bodies)	Moderate platyspondyly with anterior beaking of vertebral borders of dorsolumbar spine
Metaphyseal changes	Yes (widespread)	Yes	Yes (broadened and irregular)	Yes	-	Long bones showed relatively large epiphyses and widening, with some irregularity of the metaphyses. Metaphyseal irregularity of metacarpals/metatarsals
Other radiological findings	-	Slender bones with thin cortices, mild bowing of femur, small irregular femoral heads	-	Short metacarp and metatarsal + disostosis peripheral	Mild thoracic scoliosis, lumbar hyperlordosis, short pedicles of the lumbar spine, very mild flaring of the metaphyses and mild genu valgum. Growth plate of knee was prematurely fused, radius and ulna mildly bowed; short broad phalanges and metacarpals (especially 3-5th), all prematurely fused	Prominent deltoid tuberosities of the humeri, short and broad phalanges, ilia short with flaring of the iliac wings, vertebral alterations less prominent and restricted to the thoracic region with mild shortening of the pedicles of her lumbar spine. Pelvic radiograph showed minor irregularity of the acetabula
Bone age	Delayed	NA	NA	No delay (9 years at calendar age of 9)	Advanced (+2.6 SD)	Within normal limits
Bone density	Normal	NA	Normal	NA	NA	NA
Suggested diagnoses prior to genetic diagnosis	Spondylometaphyseal dysplasia (SMD)-type not classified	Spondylometaphyseal dysplasia (SMD)-type not classified and Osteogenesis Imperfecta type 1	Spondylometaphyseal dysplasia (SMD)-type not classified	Pseudoachondroplasia	Similar to AMDM but with milder radiological phenotype, no cone-shaped epiphyses in the hands and relatively mild mesomelia	-
Other information	-	Multiple fractures (arm as infant, wrist aged 8y, wedge T6 vertebra), blue sclerae	-	Constipation, umbilical hernia in the past (now normal), hypertrichosis	-	Hirsutism, prominent costochondral cartilages, sternal prominence, widening of wrists, genu varum
Cardiovascular	-	-	-	Normal	Complete atrioventricular block (Mobitz IIa)	-
Treatment	Good response seen in 6m GH trial aged 14 and a half years. During this time his annual growth velocity increased significantly (3.4 to 7.6 cm/yr).	Pamidronate	Successful trial of Growth Hormone (treatment ongoing) and showing good response (currently 4.6 cm/year).	Somatropin injections (3 months)	Femoral and humeral limb lengthening	-
Sequencing method	Sanger sequencing	150 bp paired end sequencing on HiSeqX as part of 100K Genomes Project, Truseq PCR-Free High Throughput library. Sequenced with parents as quod.		Exome sequencing as described previously (PMID: 33559681)	Trio exome sequencing using Sure Select Human All exon V6 targeted capture (Agilent Technologies), paired-end 150 bp sequencing on NovaSeq6000	Nextera Expanded exome kit (Illumina) and paired-end 100 bp sequencing on a HiSeq2000
Genetic testing prior to WGS/exome	-	*COL1A1/COL1A2* testing detected *COL1A1:* NM_000088.4:c.1770del; p.(Glu591Serfs*175) *de novo*. Normal karyotype.	Array CGH (60K), *SHOX* sequencing and MLPA all normal	-	Custom-designed NGS skeletal dysplasia panel (327 genes)	-

SUPPLEMENTARY INFORMATION

Variable skeletal phenotypes associated with biallelic variants in *PRKG2*

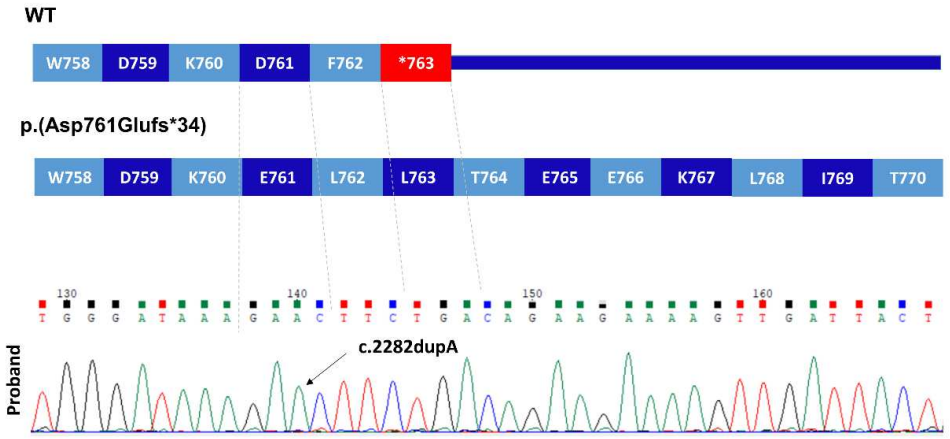

Figure S1: Sanger sequencing electropherogram validating the *PRKG2* variant in Family 1 NM_006259.3: c.2282dupA; p.(Asp761Glufs*34) which lies close to the wild-type C-terminus. Heterozygosity in parental samples was already confirmed by WGS.

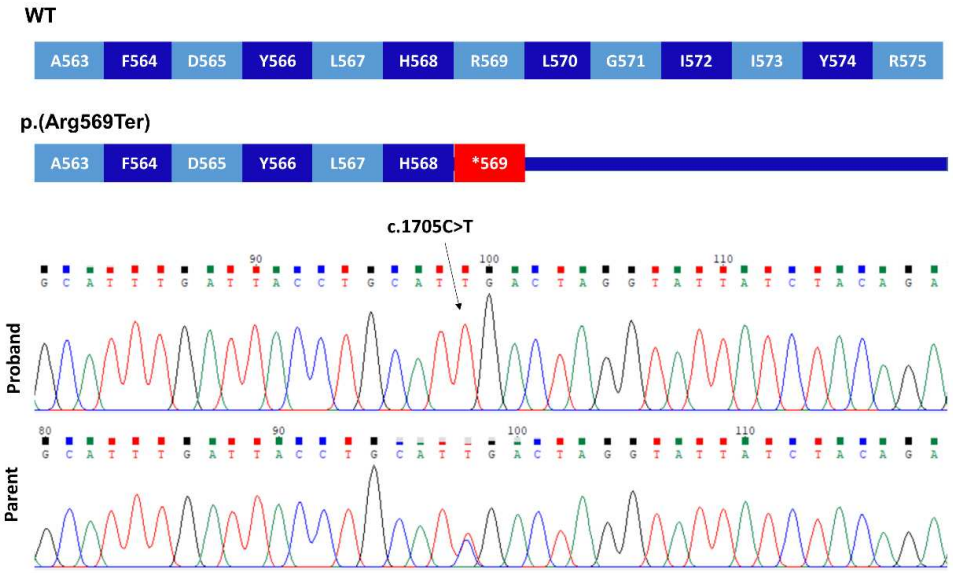

Figure S2: Sanger sequencing electropherogram showing the *PRKG2* variant in Family 2 NM_006259.3: c.1705C>T; p.(Arg569*) to be homozygous in the proband and heterozygous in a parental sample.

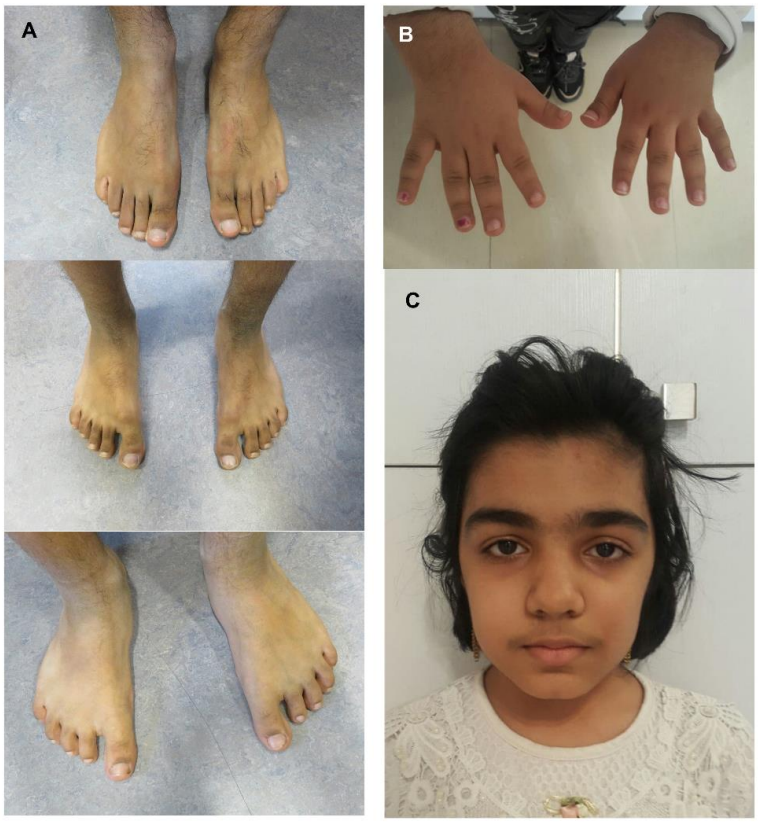

Figure S3: Photos showing clinical features of note. A) Photo showing of the toes in Family 1 which were unremarkable for F1-IV-3 (top) and F1-IV-6 (middle), but with mild shortening seen for F1-IV-7 (bottom). B) Photo showing short/broad fingers in individual F2-V-3 (aged 10 years). C) Photo showing subtle dysmorphic features in F2-V-3, with thick eyebrows, synophrys and a broad nasal bridge.

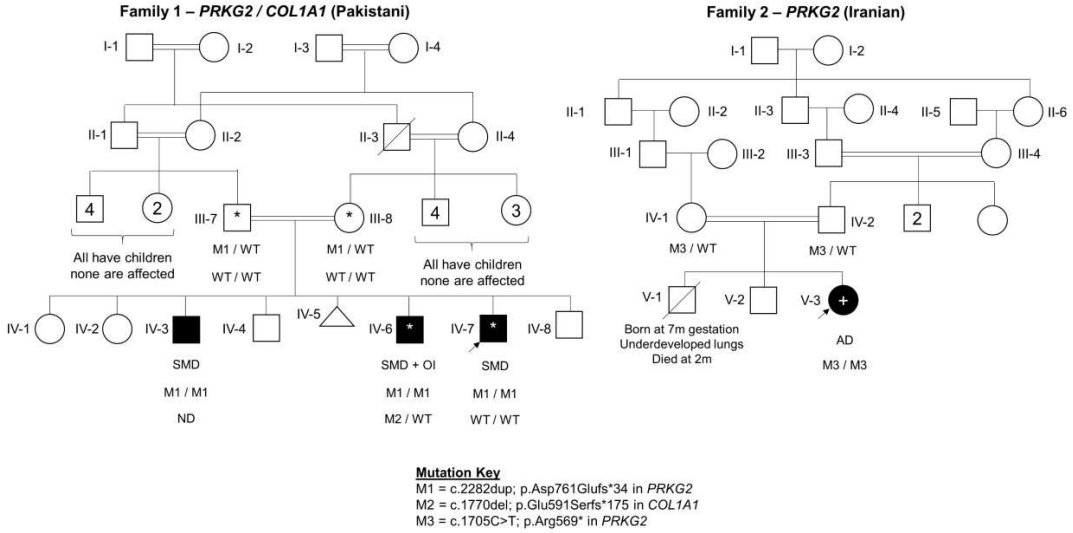

Figure S4: Full pedigrees and segregation of variants in *PRKG2* and *COL1A1* for 2 families with rare skeletal dysplasias. Pedigrees are shown in same order as the simplified versions in Figure 1A. SMD, Spondylometaphyseal dysplasia; OI, Osteogenesis imperfecta; AD, Acromesomelic dysplasia (mild); WT, wild-type; ND = not determined; *, genome sequencing performed as part of 100KGP, +, exome sequencing.

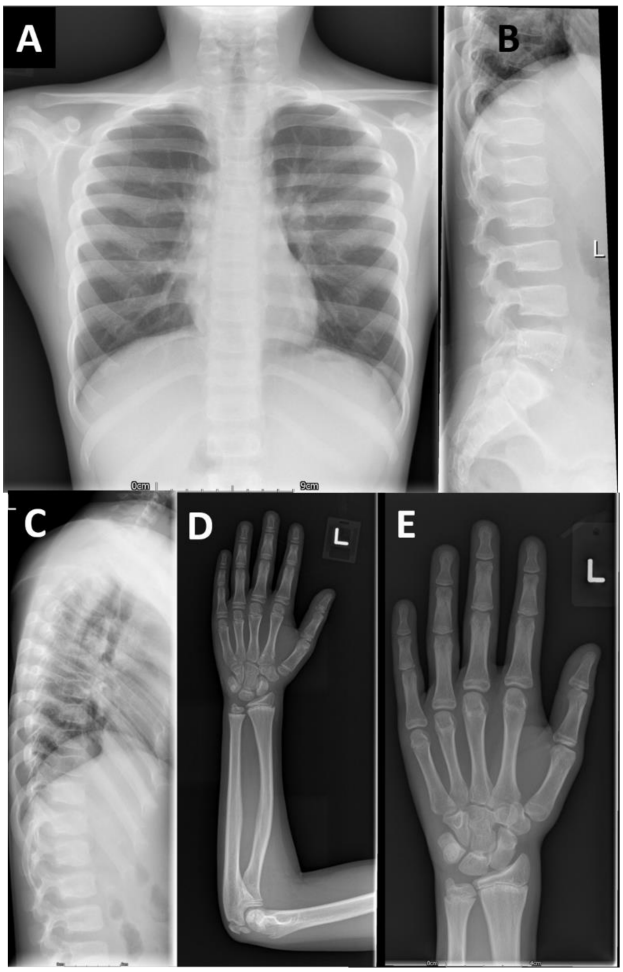

Figure S5: Additional radiological images for individual F1-IV-3. A) Chest radiograph aged 13; normal appearances. Lateral lumbar spine (B) radiograph and lateral thoracic spine radiograph aged 13. There is mild generalised platyspondyly with more pronounced height reduction in the dorsal aspects of the vertebral bodies. D) Hand and forearm aged 13. E) Hand and wrist aged 18; there is no brachydactyly.

Supplementary Methods

In silico modelling of PRKG2 frameshift variant

This composite model of the cGMP-dependent protein kinase 2 was obtained by combining several parts. The kinase domain was predicted by I-Tasser[1], while the cGMP binding domains were the crystal structures PDB:5C6C and PDB:5BV6.[2] The *in silico* calculations were done with Pyrosetta.[3] Further details and the full code is available at https://github.com/matteoferla/PRKG2_analysis. The interactive version of the model is provided using the MichelaNGLo tool.[4]

Plasmid construction

The empty Myc-DDK-tagged expression pCMV6-Entry plasmid as well as the human *PRKG2* (NM_006259.2; pCMV6-PRKG2-WT) wild type plasmids were obtained from Origene Technologies (Rockville, MD). The PRKG2 p.R569* mutant was generated as previously reported.[5] The p.D761Efs*34 mutant was generated by two sequential PCRs in order to add the extra nucleotide sequence to the C-terminus of the wild type sequence. The PCR-1 primers were 5' CCGCCGCGATCGCCATGGGAAATGGTTCAGTGAAACCTAAACATTCTA-AGCACCCAGATGGACAC3' (forward) and 5' CTTCTGTAGAGTACAGGCAGTAATCAACTTTT-CTTCTGTCAGAAGTTCTTTATCCCAGCCTGATAGC 3´ (reverse). The product of PCR-1 was then submitted to a second PCR (PCR-2) to add the remaining nucleotides to complete the mutated sequence. The same forward primer was used in PCR-2 whilst 5' GTACGCGTTAATACTCTGAAAAGAAAATAATGTGTTGGATTATTG-ATCCTTGAGGTCCTCTTCTGTAGAGTACA 3´ was employed as the reverse primer. The PCR product was then cloned into a pCR2.1 vector by TA cloning method following manufacturer´s instructions (Life Technologies, Carlsbad, CA). Next, the cloned fragment was subcloned into pCMV6 vector using the pCMV6-PRKG2-WT construct digested with SgfI and MluI enzymes (Thermo Fisher Scientific) resulting in the pCMV6-PRKG2-D761Efs*34 mutant plasmid. The construct was verified by Sanger sequencing.

MAPK pathway analysis

Cell culture, transient transfections, Western blots and densitometry quantification were performed as previously described.[5]

Table S1: Variant interpretation using ACMG guidelines.[6]

Family ID	Family 1	Family 2
Variant	NM_006259.3:c.2282dup p.(Asp761Glufs*34)	NM_006259.3:c.1705C>T p.(Arg569*)
ACMG evidence codes	PVS1 (applied with caution as near 3' end but N.B. 33 additional residues and WB data in Fig 1C,D supports use), PS3 (MAPK signalling affected, Fig 1E,F), PM2 (absent in gnomAD), PP1 (cosegregation, Fig 1A), PP3 (structural modelling, Fig 1B)	PVS1, PS3 (Diaz-Gonzalez *et al*[5] and now replicated), PM2 (singleton allele in gnomAD 2.1.1), PP3 (*in silico* e.g. CADD=37)
ACMG classification	Pathogenic	Pathogenic

Table S2: Clinical details and variant information for four individuals from two independent families with biallelic variants in *PRKG2*. Results are compared to two cases reported by Díaz-González et al 2020.[5] Sequencing methods in Family 2 are as described by Pagnamenta *et al* 2021.[7] NA, not available; ROH, region of homozygosity. Variant annotation is based on NM_006259.3. SDs for adults heights were calculated using https://tall.life/height-percentile-calculator-age-country. For Family 1 we used the mean adult height obtained from the Royal College of Paediatrics and Child Health's standard growth chart

N.B. This table is provided as a separate xlsx file.

References

1 Yang, J. & Zhang, Y. I-TASSER server: new development for protein structure and function predictions. *Nucleic Acids Res* **43**, W174-181, doi:10.1093/nar/gkv342 (2015).

2 Campbell, J. C. *et al.* Structural Basis of Cyclic Nucleotide Selectivity in cGMP-dependent Protein Kinase II. *J Biol Chem* **291**, 5623-5633, doi:10.1074/jbc.M115.691303 (2016).

3 Chaudhury, S., Lyskov, S. & Gray, J. J. PyRosetta: a script-based interface for implementing molecular modeling algorithms using Rosetta. *Bioinformatics* **26**, 689-691, doi:10.1093/bioinformatics/btq007 (2010).

4 Ferla, M. P., Pagnamenta, A. T., Damerell, D., Taylor, J. C. & Marsden, B. D. MichelaNglo: sculpting protein views on web pages without coding. *Bioinformatics* **36**, 3268-3270, doi:10.1093/bioinformatics/btaa104 (2020).

5 Diaz-Gonzalez, F. *et al.* Biallelic cGMP-dependent type II protein kinase gene (PRKG2) variants cause a novel acromesomelic dysplasia. *J Med Genet*, doi:10.1136/jmedgenet-2020-107177 (2020).

6 Richards, S. *et al.* Standards and guidelines for the interpretation of sequence variants: a joint consensus recommendation of the American College of Medical Genetics and Genomics and the Association for Molecular Pathology. *Genet Med* **17**, 405-424, doi:10.1038/gim.2015.30 (2015).

7 Pagnamenta, A. T. *et al.* An ancestral 10-bp repeat expansion in VWA1 causes recessive hereditary motor neuropathy. *Brain* **144**, 584-600, doi:10.1093/brain/awaa420 (2021).